Radio Science, Volume 34, Number 5, Pages 1217–1225, September–October 1999

Determining polarization parameters and angles of arrival of HF radio signals using three mutually orthogonal antennas

E. L. Afraimovich, V. V. Chernukhov, V. A. Kobzar, and K. S. Palamartchouk

Institute of Solar-Terrestrial Physics, Irkutsk, Russia

Abstract. This paper presents results of an experimental verification of our earlier suggested spectral-polarization method of measuring the polarization parameters and angles of arrival of HF electromagnetic waves by analyzing three mutually orthogonal projections of the radio signal field vector using a single receiving antenna. The initial stage of analysis involves calculating complex Doppler spectra of time variations of these projections. Thereupon, for each spectrum component, these data are used to determine polarization parameters and angle-of-arrival spectra. The measurements were made on a HF radio path about 100 km in length, with simultaneous monitoring of the ionospheric situation using the oblique-incidence sounding chirp-ionosonde. In an effort to eliminate multipath effects, in the analysis we used nighttime intervals, for which a stable one-mode reflected radio signal was observed. It is shown that the proposed method gives mean values of the azimuth and zenith angle which differ by no more than 2°–5° from calculated values. Results of an experimental verification of the suggested technique are in agreement with published data obtained by classic methods.

1. Introduction

Of great interest in the context of obtaining information about ionospheric conditions, as well as of improving the effectiveness of exploitation of a radio system's energy potential, is the development of diagnostic tools based on measuring the full field vector of the radio wave (angle of arrival, and polarization parameters of the electromagnetic wave (EMW)). *Morgan and Evans* [1951] described a method to determine the full EMW field vector from monostatic measurements of the received radio signal amplitudes and phases based on using three mutually orthogonal antennas. This technique makes possible a substantial reduction in size of the antenna array aperture required to determine the EMW angles of arrival. Furthermore, it eliminates errors of measurement of polarization parameters caused by an arbitrary (in the general case) orientation of the wave front with respect to the aperture plane of the antenna array. A practical implementation of the method is used in VLF radio sounding of the magnetosphere [*Calvert et al.*, 1995].

An experimental verification of the method on HF radio paths is therefore of utmost importance, but these authors are unaware of such work. The objective of this paper is to suggest a convenient (for numerical calculation) method to determine polarization parameters and angles of arrival of the EMW front based on measurements at one point of three mutually orthogonal projections of the field vector, and to present

Paper number 1999RS900042.
0048-6604/99/1999RS900042$11.00

data of an experimental verification of the technique on a short HF radio path.

In section 2, we offer a brief description of the method of measuring full field vector parameters using three mutually orthogonal antennas, basically following the initial method described in a pioneer paper [*Morgan and Evans,* 1951]. Section 3 gives a description of the experimental and data processing configuration, and section 4 presents results of an experimental verification of the method on a short HF radio path.

2. Determining Parameters of the Polarization and Angles of Arrival From Three Mutually Orthogonal Components of the Field Vector

Morgan and Evans [1951] solved the problem of determining parameters of the polarization ellipse (a is the semi-major axis, r is the ratio of the semiaxes of the incident wave, and β is the rotation angle of the ellipse's semi-major axis) and the orientation angles of a normal to the plane of the wave front (zenithal θ, and azimuthal φ) from the known amplitudes (E_1, E_2, E_3) and phases (γ_1, γ_2, γ_3) of three mutually orthogonal projections (components) of the field vector (e_1, e_2, e_3)

$$\begin{aligned} e_1 &= E_1 \sin(\omega t + \gamma_1) \\ e_2 &= E_2 \sin(\omega t + \gamma_2) \\ e_3 &= E_3 \sin(\omega t + \gamma_3) \end{aligned} \tag{1}$$

where ω is the circular frequency and t is the time. *Morgan and Evans* [1951] suggested that parameters of the polarization be determined graphically from nomograms, which gives no way of employing this technique in numerical calculations. An algorithm that is free from such limitations is considered below.

We use rectangular coordinate systems [*Morgan and Evans,* 1951], in which we will seek the solution of the problem (Figure 1). The 123 coordinate system has axes $O1$, $O2$, and $O3$. The xOy coordinate system is specified in the plane of the wave front of the incident wave (the axis Oy is determined by the intersection of the plane passing through the axis $O3$ and a normal to the wave front, with the plane of the wave front, and the axis Ox is orthogonal to Oy and parallel to the plane $1O2$). The $x'Oy'$ coordinate system is formed by the axes Ox', Oy' (by the projection of the axes Ox, Oy onto the plane $1O2$).

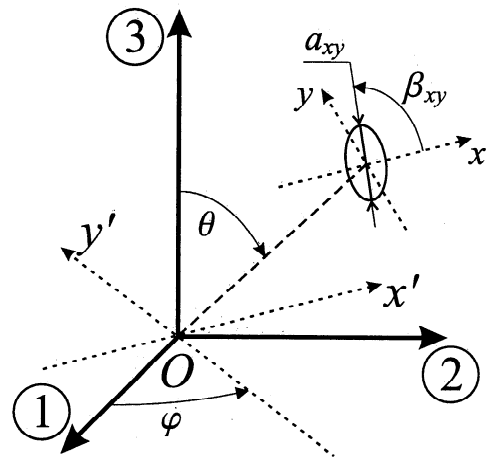

Figure 1. Geometry of the solution of the problem of determining polarization parameters. The coordinate systems 123, xOy, and $x'Oy'$ are plotted. The arrival direction of the wave front is specified by the zenith angle θ (measured from the axis $O3$) and the azimuth φ (measured from the axis $O1$ toward axis $O2$), the rotation angle of the major semiaxis of the polarization ellipse β_{xy} (measured from the axis Ox).

The arrival direction of the wave front is specified by the zenith angle θ (measured from the axis $O3$) and the azimuth φ (measured from the axis $O1$ toward axis $O2$).

First we determine the angle of arrival of the wave as described by *Morgan and Evans* [1951]:

$$\begin{aligned} \tan\varphi &= \frac{E_1 \sin(\gamma_1 - \gamma_3)}{E_2 \sin(\gamma_3 - \gamma_2)} \\ \tan^2\theta &= \frac{E_1^2 E_3^2 \sin^2(\gamma_1 - \gamma_3) + E_3^2 E_2^2 \sin^2(\gamma_3 - \gamma_2)}{E_2^2 E_1^2 \sin^2(\gamma_2 - \gamma_1)} \end{aligned} \tag{2}$$

Further, using the relationships from *Kanareikin et al.* [1966], we determine the semiaxes ratio r_{12} and the rotation angle β_{12} of the semi-major axis of the wave's polarization ellipse projected onto the plane $1O2$. Figure 2 illustrates the situation in this plane.

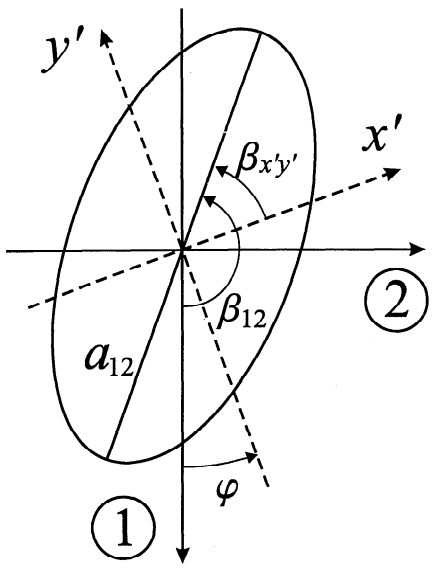

Figure 2. Geometrical relationships when determining the rotation angle $\beta_{x'y'}$ of the projection of the polarization ellipse of the incident electromagnetic wave in the plane $x'Oy'$ relative to the axis Ox'. β_{12} is rotation angle of the projection of the major semiaxis of the polarization ellipse onto the plane $1O2$ relative to the axis $O1$.

$$\beta_{12} = \frac{1}{2}\arctan\frac{2E_1E_2\cos(\gamma_1-\gamma_2)}{E_1^2-E_2^2}$$
$$r_{12} = \Big[\Big(E_1^2\sin^2\beta_{12} + E_2^2\cos^2\beta_{12} - E_1E_2\sin 2\beta_{12}\cos(\gamma_1-\gamma_2)\Big)\Big/ \Big(E_1^2\cos^2\beta_{12} + E_2^2\sin^2\beta_{12} + E_1E_2\sin 2\beta_{12}\cos(\gamma_1-\gamma_2)\Big)\Big]^{1/2} \quad (3)$$

Hence the parameters β_{12} and r_{12} model observations from a conventional polarimeter with two mutually perpendicular antennas. An analysis of the geometry of Figures 1 and 2 reveals that $\beta_{x'y'} = \beta_{12} - (\varphi + 90°)$, $\delta_{x'y'} = \delta_{xy}$, and $E_x = E_{x'}$.

An inverse transformation of the projection parameters of the wave's polarization ellipse onto the plane $x'Oy'$ into the amplitudes and phase difference of the mutually orthogonal field components in this same plane is performed by [*Morgan and Evans,* 1951]

$$E_{x'} = a_{12}\sqrt{\cos^2\beta + r^2\sin^2\beta}$$
$$E_{y'} = a_{12}\sqrt{\sin^2\beta + r^2\cos^2\beta} \quad (4)$$
$$\delta_{x'y'} = \gamma_1 - \gamma_2 = \arctan\frac{2r}{(1-r^2)\sin 2\beta}$$

where a a_{12} is the semimajor axis of the projection of the polarization ellipse, which plays the role of a scale factor; its absolute value is unimportant.

Therefore, on substituting a_{12} for $a_{x'y'}$ and β for $\beta_{x'y'}$ in (4), we obtain set ($E_{x'}$, $E_{y'}$, and $\delta_{x'y'}$) instead of set (E_1, E_2, and δ_{12}). Alternatively, from geometrical considerations, $E_y = E_3\sin\theta$. Thus we have obtained the amplitudes (E_x, E_y) and phase difference (δ_{xy}) of the mutually orthogonal projections of the field vector in the plane of the wave front.

Substituting E_x, E_y, and δ_{xy} into (4) gives the expressions for the polarization ellipse parameters in the plane of the wave front:

$$\beta_{xy} = \frac{1}{2}\arctan\frac{2E_xE_y\cos\delta_{xy}}{E_x^2-E_y^2}$$
$$r_{xy} = \Big[\Big(E_x^2\sin^2\beta + E_y^2\cos^2\beta - E_xE_y\sin 2\beta\cos\delta_{xy}\Big)\Big/ \Big(E_x^2\cos^2\beta + E_y^2\sin^2\beta + E_xE_y\sin 2\beta\cos\delta_{xy}\Big)\Big]^{1/2} \quad (5)$$

It is along this pathway that by using suitably chosen coordinate systems and equations (2)–(5) it is possible to solve the problem of determining the parameters of the polarization ellipse in the plane of the EMW wave front from three mutually orthogonal components of the field vector.

Morgan and Evans [1951] developed a method to analyze and synthesize a three-component field for the one-mode signal. An extension of the method from *Morgan and Evans* [1951] to the case of a multimode radio signal was suggested by *Afraimovich* [1982] and *Afraimovich and Palamartchouk* [1998], implying a spectral-polarization technique for analyzing the full vector of the radio wave field, based on complex Doppler mode filtering. The essence of the method is that in all algorithms for computing

parameters (2)–(5) of the field's full vector using systems of equations for mutually orthogonal projections of the field, in lieu of complex amplitudes of projections (e_1, e_2, e_3), complex amplitudes of complex Doppler spectrum components of these projections are used, that is, amplitude $S_1(\Omega)$, $S_2(\Omega)$, $S_3(\Omega)$ and phase $\Phi_1(\Omega)$, $\Phi_2(\Omega)$, $\Phi_3(\Omega)$ spectra, where ω is the circular frequency of spectrum components:

$$\begin{array}{ll} E_1(\Omega) = S_1(\Omega) & \gamma_1(\Omega) = \Phi_1(\Omega) \\ E_2(\Omega) = S_2(\Omega) & \gamma_2(\Omega) = \Phi_2(\Omega) \\ E_3(\Omega) = S_3(\Omega) & \gamma_3(\Omega) = \Phi_3(\Omega) \end{array} \quad (6)$$

These spectra are calculated for complex amplitudes of the output signal from corresponding mutually orthogonal antennas using fast Fourier transform (FFT) algorithms and suitable time and spectral windows. Not only does complex Doppler filtering make it possible to separate the interfering modes, but it also enhances noise immunity of measurements and hence the stability of the solution of (2)–(5).

In actual practice, EMW angles of arrival and polarization parameters are determined in the presence of noise. The method proposed, however, does not permit the noise influence upon the accuracy of measurement of these parameters to be taken into account in analytical form. Therefore a numerical simulation was carried out in order to estimate the noise influence upon the reconstruction accuracy of the full field vector [*Afraimovich and Palamartchouk,* 1998]. This was done in the following way: first we generated series of simultaneous counts of the field vector projections $e_1(t)$, $e_2(t)$, $e_3(t)$ of the EMW arriving from a given direction within one octant. Thereupon these series were subjected to a direct Fourier transform. Next we calculated for each of the spectral components the full field vector parameters by (2)–(5).

The rms of reconstructed parameters was taken to be the measurement accuracy index. Thus, by estimating the effectivenes of measuring polarization parameters and angles of arrival of the EMW at different noise levels, it has been shown that in the greater part of the octant, with the signal-to-noise ratio not worse than 1.0, the errors of determining the angles of arrival (θ and φ), the axes ratio r of the polarization ellipse, and the rotation angle β of ellipse's semiaxis do not exceed 0.5°, 0.08, and 8°, respectively.

3. General Description of the Experiment, and Data Pretreatment

For an experimental verification of the method, a special-purpose facility was installed at the Institute of Solar-Terrestrial Physics research range near Irkutsk (52°N, 104°E), Russia, which is designed for measuring and recording complex amplitudes of three mutually orthogonal projections of the full vector of the radio wave field. The measurements were made on a path 113 km in length, with the geographical azimuth 64°, by sounding with a continuous HF radio signal at the sounding frequency $f = 3.13$ MHz.

The particular working frequency was determined based on average data of oblique-incidence ionospheric sounding to correspond to the middle point of the path for selected time interval. These measurements were carried out every hour with the chirp-ionosonde described by *Brynko et al.* [1988]. Most data were obtained for the nighttime, when reflection was from the ionospheric F_2 region. To illustrate experimental results, we selected a typical time interval, from 1500 to 2200 UT on June 25, 1997 (from 2200 LT on June 25 to 0500 LT on June 26).

Figure 3 presents frequency dependences of the effective reflection height $H(f)$ of the HF radio signal (ionograms) measured on June 25, 1997, from 1501 to 1601 UT with the chirp-ionosonde. The vertical bars show the value of the sounding frequency.

It should be noted that in Figure 3 the information about the frequency dependence $H(f)$ of first- and second-multiplicity signals is plotted by black and grey points, in order to show that second-multiplicity signals in these measurements are an order of magnitude weaker. Furthermore, despite the relative proximity of

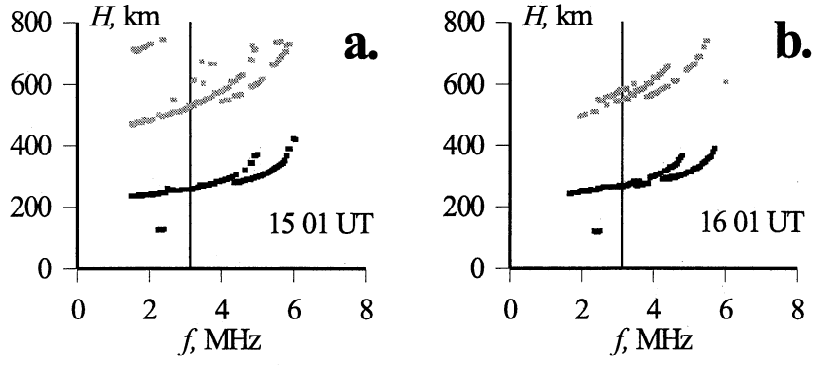

Figure 3. Chirp-ionosonde ionograms taken on June 25, 1997, (a) at 1501 UT; (b) at 1601 UT. Vertical bars show the value of the sounding frequency of 3.13 MHz.

the transmitter, we were also able to neglect the influence of the ground wave because its additional attenuation was caused by a mountain range between the reception facility and the transmitter. In the first approximation, we can therefore conceive of the measurements as being made for the one-ray (one-mode) radio signal. It is evident from Figure 3 that the ordinary component of the reflected signal was typically recorded at the selected sounding frequency, and corresponding values of the effective height were determined for the selected time interval in the range from 230 to 270 km.

The antenna-feeder system, consisting of three mutually orthogonal magnetic antennas (1, 2, and 3) and the antenna switch, converted the electromagnetic wave energy to electrical signals proportional to projections of the full vector of the wave field. Phase calibration of the antenna-feeder system was done by feeding the calibration signal simultaneously to all cable inputs of the reception system (instead of the signal from the antennas); phase corrections, calculated for each of the working frequencies of the range, were entered into a personal computer and were taken into account in the processing.

We used special-purpose direction-finder cavity magnetic antennas to receive signals only from the upper hemisphere by screening secondary signals reflected from the terrestrial surface. Magnetic dipoles were aligned along the axes of the antenna frame of reference (system 123) in such a manner as shown in Figure 4 by bold line segments. In the geographical coordinate system (system $X0Y$), the axes Z, Y, X are pointing to the zenith, to the north N, and to the east E, respectively; $\boldsymbol{k}$ is the wave vector in the above coordinate systems. The arrival direction of the wave front is specified by the zenith

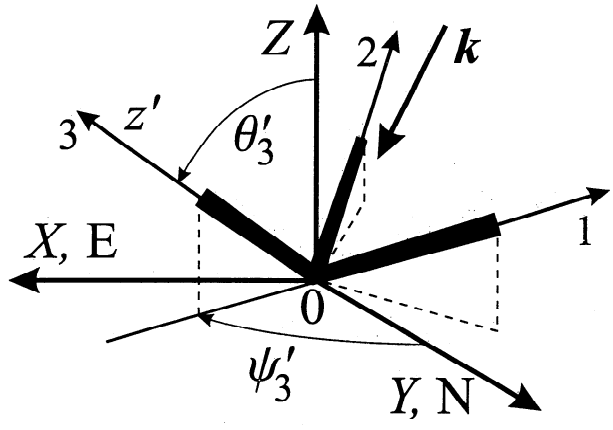

Figure 4. Frame of reference (system 123) of the three-component antenna, and geographical coordinate system ($X0Y$). In the geographical coordinate system, the axes Z, Y, and X are pointing to the zenith, to the north N, and to the east E, respectively. Here $\boldsymbol{k}$ is the wave vector in the above coordinate systems; ψ' and θ' are corresponding angular coordinates of all the projections of the three-component antenna. The figure also shows the angular coordinates ψ'_3 and θ'_3, corresponding to the third projection of the three-component antenna.

angle θ' (measured from the axis OZ) and the azimuth ψ' (measured from the axis OY toward axis OX). Figure 4 also shows the angular coordinates ψ'_3 and θ'_3, corresponding to the third projection of the three-component antenna.

A calculation of the expected zenith angle θ'_0 for this path using the data from the chirp-ionosonde based on Martin's theorem from the familiar relationships [*Davies,* 1969] showed that $\theta'_0 = 10°$–$12°$. Therefore the best choice from the point of view of the attenuation of interference effects caused by reflection from the terrestrial surface and from surrounding objects was an orientation of the antennas' coordinate system where the symmetry axis of the three-component antenna was pointing to zenith. Results presented below were obtained for the same values of $\theta' = 55°$; $\psi'_1 = 240°$, $\psi'_2 = 120°$, and $\psi'_3 = 0°$.

At the first stage of data processing, the series obtained (equation (1)) were fast-Fourier transformed with the length of a series of 512 counts, which corresponded to the integration time of about 32 s and a frequency resolution of 0.03 Hz. The particular length of the series was determined by the required time resolution of a secondary data processing in order to determine the angles of arrival and polarization parameters. Of course, this led to a decrease in frequency resolution of the various modes of the reflected signal. However, as has been pointed out above, in the analysis we used time intervals predominantly with a one-ray signal, so that this impairment did not affect our final results.

The series of amplitude $S_1(\Omega)$, $S_2(\Omega)$, $S_3(\Omega)$ and phase $\Phi_1(\Omega)$, $\Phi_2(\Omega)$, $\Phi_3(\Omega)$ spectra in the design of the proposed algorithm are results of a data pretreatment; a further analysis of the signal, however, was carried out in a complex Fourier domain. Depending on the tackled problem, different algorithms for a secondary processing of these series may be suggested. For our chosen variant with a one-ray signal, it was best to simply average the amplitude and the phase difference for those spectral components whose amplitude was higher than the specified relative threshold ε (in our case, $\varepsilon = 0.9$), followed by the determination of the angles of arrival and of the polarization parameters using (2)–(5).

Then angles of arrival φ and θ and the rotation angle of the ellipse axes β_{12} are converted from the antenna's frame (system 123) of reference to the geographical coordinate system ($X0Y$), using the familiar formulae of rotation of the Cartesian coordinate system. New notations of this parameters are ψ', θ', and β'.

4. Measuring Parameters of the Polarization and Angles of Arrival Using a Three-Component Antenna

In Figure 5, we present time dependencies (Figures 5a and 5b) and histograms (Figures 5e and 5f) of the azimuth $\psi'(t)$ and zenith angle $\theta'(t)$ in the geographical coordinate system which were measured on June 25, 1997, from 1500 to 2200 UT and smoothed with the 5-min time window. Horizontal bars show the true value of the azimuth $\psi'_0 = 64°$ and the calculated value of the zenith angle $\theta'_0 = 11°$.

For the selected time interval presented in Figure 5, the mean values and the rms of the azimuth $\psi'(t)$ in the geographical coordinate system were 70° and 14°, respectively, (Figure 5a), and those of the zenith angle $\theta'(t)$ were 8.2° and 2.7°, respectively, (Figure 5b).

As can be made certain, the estimated mean value of the zenith angle is less than the calculated value by no more than 2°–3° and that of the azimuth is larger than the calculated value by 6°. Considering the fact that the accuracy of installation of the platform with a three-component antenna with respect to the geographical coordinate system did not exceed a few degrees, such a result may be regarded as a quite convincing validation of the proposed method for determining angles of arrival.

In regard to angle-of-arrival variations whose amplitude can be inferred from corresponding rms values, they correlate quite well with published data obtained on short-range HF paths using conventional methods of angle-of-arrival

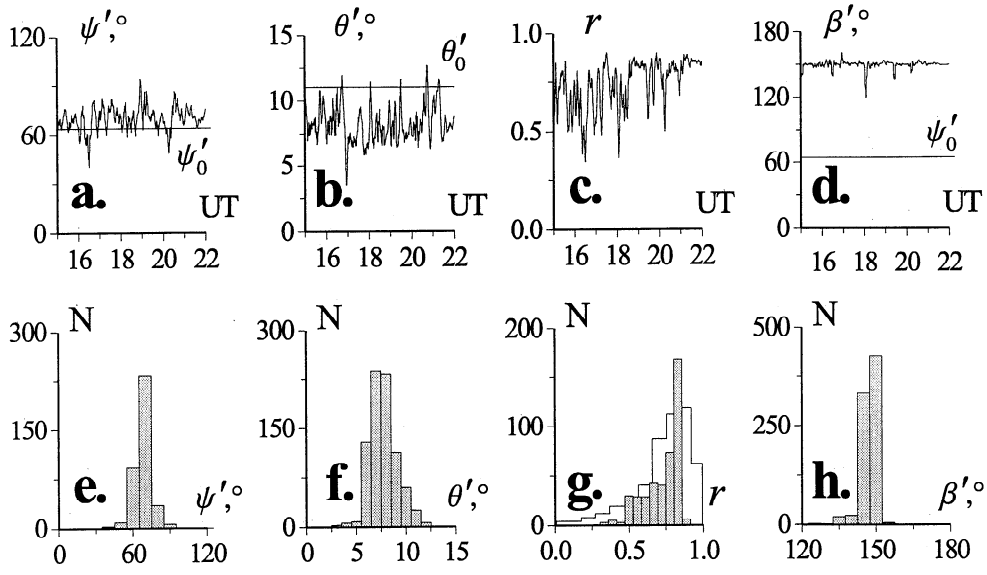

Figure 5. (a and b) Time dependences and (e and f) histograms of the azimuth $\psi'(t)$ and zenith angle $\theta'(t)$ in the geographical coordinate system measured on June 25, 1997, from 1500 UT to 2200 UT and smoothed with the 5-min time window. Horizontal bars on Figures 5a and 5d show values of the actual azimuth to the transmitter (64°) and of the zenith angle (11°), calculated based on ionospheric sounding data from the chirp-ionosonde. The figure shows (c and d) time dependences and (g and h) histograms of the measured ratios of the ellipse axes r and of the rotation angle of the ellipse axes β' in the geographical coordinate system $(X0Y)$. The difference between $\beta'(t)$ and ψ'_0 averages 86°. The line in Figure 5g represents the histogram of the measured ratios of the ellipse axes at 5-MHz frequency made on a 100-km-long path using a conventional polarimeter [*Afraimovich et al.*, 1988].

measurement [*Reynolds and Morgan,* 1975; *Jones and Reynolds,* 1975; *Walton and Bailey,* 1976; *Lyon,* 1979; *Afraimovich,* 1982; *Tedd et al.,* 1984; *Afraimovich et al.,* 1985].

It should be noted that oscillations with typical periods between 10 min and 1 hour are especially pronounced in angle-of-arrival variations. It is commonly believed that these oscillations are caused by medium-scale traveling ionospheric disturbances, forming the basis for appropriate methods of monitoring these disturbances in spaced antenna reception with a small baseline [see, for example, *Reynolds and Morgan,* 1975; *Jones and Reynolds,* 1975; *Walton and Bailey,* 1976; *Lyon,* 1979; *Afraimovich,* 1982; *Tedd et al.,* 1984; *Afraimovich et al.,* 1985].

Results of measurements of the polarization ellipse parameters for a similar time interval are also presented in Figure 5. The figure shows time dependences of the measured ratios of the ellipse axes $r(t)$ (Figure 5c) and of the rotation angle of the ellipse axes $\beta'(t)$ (Figure 5d) in the geographical coordinate system $(X0Y)$, and histograms of these parameters (Figures 5g and 5h). The mean values and the rms of the ratio r of the polarization ellipse axes are 0.74 and 0.12, respectively, and those of the rotation angle β' of the polarization ellipse are 150° and 4°. The line in Figure 5g represents the histogram of the measured ratios r of the ellipse axes at 5-MHz frequency made on a 100-km-long path using a conventional polarimeter [*Afraimovich et al.,* 1988], which is similar in its form to the

histogram for the case of three-component measurements. About 0.5 of the measured values of the ellipse semiaxes ratio are in the range 0.75–0.9 in both experiments.

Measurements of the sign of rotation of the polarization vector showed that for the selected time interval the relative number of runs with clockwise rotation (the ordinary component) is no less than 0.98, which is in quite good agreement with results of ionogram analysis (Figure 3).

Thus an almost circularly polarized signal was recorded in the present case. As would be expected for this situation, the rotation angle β' of the principal axis of the polarization ellipse in a geographical coordinate system was determined not so much by the value of this quantity in the plane of the wave front as by the azimuth of the radio path, and it differed from the value of ψ' by 90°. Indeed, the difference between $\beta'(t)$ and ψ'_0 averages 86° for our experiment, which approaches the expected value.

5. Conclusions

Experimental results have shown that the proposed method gives stable mean values of the azimuth and of the zenith angle different from calculated values by no more than 2°–6°, and angle-of-arrival and polarization parameter variations are consistent with published data for short-range HF radio paths, based on classical methods of measuring these parameters.

In this case we were able to assess the validity of angle-of-arrival measurements only on the basis of the data on the radio path geometry. Because of our limited resources, we were also unable to carry out experiments aimed at a "direct" comparison of related experiments using our suggested method and existing classic facilities (HF direction finders, arrays, etc.). At some future date, it is necessary to conduct a series of comprehensive experiments using, among other things, movable platforms.

In accordance with the chief objective of our work, we restricted our analysis to the one-mode signal only, because analyzing the applicability of the method under multimode propagation conditions is a separate independent problem.

Unfortunately, for technical reasons and because of experimental conditions, the amount of experimental material suitable for processing was quite small, so it was not possible for us to obtain the necessary data for evaluating the performance of the technique under different geophysical conditions, as well as under multimode propagation conditions. We understand that such a comparison is insufficient for an adequate assessment of the attainable accuracy and reliability of results.

The use of the proposed method can improve spatial resolution in remote sensing from such mobile platforms as sea ships and satellites (also in the case of topside soundings), as well as in the configuration of classical spaced antenna reception but with the use of three-component receiving antennas. This last variant combines two independent methods for measuring angles of arrival, which affords a substantial improvement to the reliability of measurements and provides new information about, for example, the curvature of the interference pattern front.

Acknowledgments. We are indebted to V. E. Nosov and V. I. Kurkin for providing us with chirp-sounding data spanning the period of our measurements. Great contributions were made by two referees. This work was done with support from the Russian Foundation for Basic Research, grants 99–05–64753 and 97–02–96060.

References

Afraimovich, E. L., *Interference Methods of Ionospheric Radio Sounding*, Nauka, Moscow, 1982.

Afraimovich, E. L., and K. S. Palamartchouk, Determining the velocity of the interference pattern by analyzing three mutually orthogonal projections of the radio signal field vector, I, Numerical simulation, *J. Atmos. Sol. Terr. Phys., 60,* 115–120, 1998.

Afraimovich, E. L., Y. F. Ashkaliev, M. A. Belyaev, V. I. Vyborov, A. V. Lysak, and M. Y. Udodov, Variation of HF radio signal arrival angles and medium-scale travelling ionospheric disturbances, *Issled. Geomagn. Aeron. Fiz. Solntsa, 73,* 96–104, 1985.

Afraimovich, E. L., M. A. Belyaev, A. V. Lysak, On the effectiveness of polarization filtering of the HF radio

signal, *Issled. Geomagn. Aeron. Fiz. Solntsa, 81,* 25–32, 1988.

Brynko, I. G., I. A. Galkin, V. P. Grozov, N. I. Dvinskikh, S. M. Matyushonok, and V. E. Nosov, An automatically controlled data gathering and processing system using an FMCW ionosonde, *Adv. Space Res., 8,* (4), 121–124, 1988.

Calvert, W., et al., The feasibility of radio sounding in the magnetosphere, *Radio Sci., 30,* 1577–1595, 1995.

Davies, K., *Ionospheric Radio Waves,* Blaisdell, Waltham, Mass., 1969.

Jones, T. B., and J. S. B. Reynolds, Ionospheric perturbations and their effect on the accuracy of h. f. direction finders, *Radio Electron. Eng., 45,* 63–72, 1975.

Kanareikin, D. B., N. F. Pavlov, and V. A. Potekhin, *The Polarization of Radar Signals,* Sov. Radio, Moscow, 1966.

Lyon, G. F., The corrugated reflector model for one-hop oblique propagation, *J. Atmos. Terr. Phys., 41,* 5–9, 1979.

Morgan, M. and W. Evans, Synthesis and analysis of elliptic polarization loci in terms of space-quadrature sinusoidal components, *Proc. IRE, 39,* 552–556, 1951.

Tedd, B. L., H. J. Strangeways, and T. B. Jones, The influence of large-scale TIDs on the bearings of geographically spaced HF transmissions, *J. Atmos. Terr. Phys., 46,* 109–117, 1984.

Reynolds, J. S. B., and A. D. Morgan, The effect of frequency separation on the correlation of bearing errors measured on ionospherically propagated HF signal from colocated transmitters, *J. Atmos. Terr. Phys., 37,* 545–551, 1975.

Walton, E, K, and A. D. Bailey, Observation of seasonal effects in traveling ionospheric disturbances by the directional deviation technique, *Radio Sci. 11,* 175–178, 1976.

E. L. Afraimovich, V. V. Chernukhov, V. A. Kobzar, and K. S. Palamartchouk, Institute of Solar-Terrestrial Physics SD RAS, P. O. Box 4026, Irkutsk, 664033, Russia. (e-mail: afra@iszf.irk.ru; kpal@iszf.irk.ru)

(Received September 18, 1998; revised March 15, 1999; accepted April 1, 1999.)